Comparison of Lipid-Binding and Lecithin:Cholesterol Acyltransferase Activation of the Amino- and Carboxyl-Terminal Domains of Human Apolipoprotein E3†

Martine De Pauw,‡ Berlinda Vanloo,‡ Karl Weisgraber,§ and Maryvonne Rosseneu*,‡

Laboratory of Lipoprotein Chemistry, Department of Biochemistry, Faculty of Medicine, University of Gent, Hospitaalstraat 13, B 9000 Gent, Belgium, and Gladstone Institute of Cardiovascular Disease, Cardiovascular Research Institute, Department of Pathology, University of California, San Francisco, California 94110

Received January 26, 1995; Revised Manuscript Received May 15, 1995⊗

ABSTRACT: To extend the characterization of the functional domains of apolipoprotein E (apoE), the amino- (residues 1−191, 22-kDa) and carboxyl-terminal (residues 216−299, 10-kDa) fragments were tested for lipid binding and lecithin:cholesterol acyltransferase (LCAT) activation. A disulfide bond linking helices 2 and 3 of the four-helix bundle amino-terminal domain was introduced by mutating threonine-57 to cysteine (Thr57→Cys) in apoE3 (cysteine at position 112) to determine the influence of the disulfide bond on the properties of this domain. Lipid-binding properties were determined by the ability to form complexes with dimyristoylphosphatidylcholine (DMPC) and dipalmitoylphosphatidylcholine, assessed by measuring decreases in turbidity as a function of temperature. The results demonstrate that the relative lipid binding efficiencies were intact apoE3 ~ 10-kDa fragment > 22-kDa fragment > Thr57→Cys variant. In addition, free, non-lipid-associated protein was observed with the two 22-kDa fragments but not with intact apoE3 or the 10-kDa fragment. The transition temperatures determined by fluorescence polarization were higher for the DMPC complexes with intact apoE3 and with 22- and 10-kDa fragments (25.5 °C) than with the 22-kDa Thr57→Cys variant (23.5 °C), suggesting that the variant fragment possessed the lowest affinity for lipid. Attenuated total reflection infrared measurements of the complexes indicated that the long axes of the α-helices of the various apoE forms were parallel to the acyl chains of the phospholipid bilayer. The substrate efficiency (V_{max}/K_m) for LCAT activation was higher for the palmitoyllinoleoylphosphatidylcholine−cholesterol complexes with the 10-kDa fragment (1.5 nmol of cholesteryl esters h^{-1} μM^{-1}) than with intact apoE3 (0.5 nmol of cholesteryl esters h^{-1} μM^{-1}). The reaction rates for the 22-kDa fragment and the Thr57→Cys variant were too low for an accurate determination of the kinetic parameters. Collectively, these data indicate that the 22-kDa fragment associates less with lipids than do intact apoE3 and the 10-kDa fragment. Moreover, the lipid binding is further decreased when two of the four helical segments of the 22-kDa fragment are linked by a disulfide bond. These observations support the concept that an antiparallel orientation of 17-residue helices provides an optimal configuration and a general mode of association for amphipathic helices within a discoidal apoprotein−lipid complex. The LCAT-activating properties of intact apoE3 are contained within the carboxyl-terminal domain.

Apolipoprotein E (apoE)[1] plays an important role in cholesterol metabolism, as it is a high-affinity ligand for the cellular LDL receptor. As such, apoE is involved in the catabolism of several lipoprotein classes, including very low-density lipoproteins (VLDL) and chylomicron remnants (Mahley & Innerarity, 1983). Discoidal phospholipid−cholesterol−apolipoprotein complexes containing apoA-I, apoA-IV, and apoE represent nascent high-density lipoproteins (HDL). They can be generated during lipolysis of triglyceride-rich VLDL or chylomicra (Eisenberg, 1984) and are also synthesized by the liver (Tall et al., 1977; Jonas, 1984). It has been proposed that discoidal complexes containing apoE can act as efficient cholesterol acceptors when apoA-I is either absent or deficient in human plasma (Gordon et al., 1983; Chen & Albers, 1985; Koo et al., 1985). These discoidal particles can subsequently be converted into spherical mature HDL under the action of lecithin:cholesterol acyltransferase (LCAT).

The primary structure of apoE has been determined both by protein sequencing (Rall et al., 1982) and by cDNA analysis (McLean et al., 1984; Zannis et al., 1984). Cys-

† M. De Pauw is a recipient of a fellowship of the I.W.O.N.L. (Instituut tot aanmoediging van het Wetenschappelijk Onderzoek in Nijverheid en Landbouw). A portion of this work was supported by NIH Program Project Grant HL 41633.

* Address correspondence to this author at Laboratory of Lipoprotein Chemistry, Department of Biochemistry, Faculty of Medicine, University of Gent, Hospitaalstraat 13, B 9000 Gent, Belgium. Telephone: +32 9 224 02 24, ext. 220. Fax: +32 9 264 53 37.

‡ University of Gent.

§ University of California, San Francisco.

⊗ Abstract published in *Advance ACS Abstracts,* July 1, 1995.

[1] Abbreviations: apo, apolipoprotein; ATR-IR, attenuated total reflection infrared spectroscopy; BSA, bovine serum albumin; CD, circular dichroism; CE, cholesteryl esters; DMPC, dimyristoylphosphatidylcholine; DPH, diphenylhexatriene; DPPC, dipalmitoylphosphatidylcholine; EM, electron microscopy; GdnHCl, guanidine hydrochloride; GGE, gradient gel electrophoresis; HDL, high-density lipoproteins; HPLC, high-performance liquid chromatography; IR, infrared spectroscopy; LCAT, lecithin:cholesterol acyltransferase; MW, molecular weight; PLPC, palmitoyllinoleoylphosphatidylcholine; SDS-PAGE, sodium dodecyl sulfate−polyacrylamide gel electrophoresis; VLDL, very low-density lipoproteins; 22-kDa fragment, amino-terminal (residues 1−191) thrombolytic fragment of apoE3; 22-kDa Thr57→Cys variant, amino-terminal (residues 1−191) portion of apoE3 with a Thr57→Cys mutation; 10-kDa fragment, carboxyl-terminal (residues 216−299) thrombolytic fragment of apoE3.

0006-2960/95/0434-10953$09.00/0

teine−arginine interchanges at residues 112 and 158 have been shown to have a major impact on its structure and function (Weisgraber et al., 1981; Rall et al., 1982; Weisgraber, 1994).

Apolipoprotein E has to be combined with phospholipids before it can bind to the LDL receptor (Innerarity et al., 1979). In order to define the location of the lipid-binding and LCAT-activating domains in apoE3, two fragments were prepared by thrombin cleavage: a 22-kDa (residues 1−191) and a 10-kDa (residues 216−299) fragment (Innerarity et al., 1983). The X-ray crystal structure of the amino-terminal domain of apoE3 revealed five helices in the 22-kDa fragment (Wilson et al., 1991). Four of the helices, containing 19 (residues 24−42), 28 (residues 54−81), 36 (residues 87−122), and 35 (residues 130−164) amino acids, respectively, are arranged as an antiparallel four-helix bundle; interestingly, while the average length of the helices in the other soluble apolipoproteins is about 17 residues (Brasseur et al., 1992), three of the helices in the amino-terminal domain of apoE3 are about twice as long (Wilson et al., 1991). A kink in helix 3 at Gly105 might create a β-turn in the presence of lipids, folding the helix into two 17-residue helices whose lengths would be more suited to spanning the phospholipid bilayer. To test this hypothesis, we compared the lipid-binding properties of the 22-kDa fragment of apoE3 and a 22-kDa Thr57→Cys variant, produced by site-directed mutagenesis in which two helices in the four-helix bundle are joined together via a disulfide bond between Cys57 (helix 2) and Cys112 (helix 3). A comparison of the lipid-binding properties of apoE3 and of the variant 22-kDa fragments indicates that conformation changes occur when these fragments associate with lipid.

EXPERIMENTAL PROCEDURES

Preparation of apoE3. Human apoE3 was isolated as described (Weisgraber et al., 1981). Briefly, $d < 1.02$ g/mL plasma lipoproteins from a subject with the apoE3/3 phenotype were isolated by ultracentrifugal flotation and delipidated in $CHCl_3$/MeOH (2:1, v/v). The protein was solubilized in 6 M guanidine hydrochloride (GdnHCl), 0.1 M Tris-HCl, pH 7.4, 0.01% EDTA, and 1% β-mercaptoethanol. The apoE was isolated by column chromatography on Sephacryl S-300 in 4 M GdnHCl, 0.1 M Tris-HCl, pH 7.4, 0.01% EDTA, and 0.1% β-mercaptoethanol. The fractions corresponding to apoE were pooled, dialyzed against 5 mM NH_4HCO_3, and lyophilized. The protein was solubilized in 0.1 M NH_4HCO_3 and stored at −20 °C. Prior to use, the protein was thawed and stored at 4 °C for at least 24 h.

Preparation of apoE3 Thrombolytic Fragments. Apolipoprotein E3 (1 mg/mL) was incubated with thrombin (2800 units/mg, 10 μg/mL) for 20 h at 20 °C in 0.1 M NH_4HCO_3. The proteolytic digest was lyophilized and then solubilized in 6 M GdnHCl, 0.1 M Tris-HCl, pH 7.4, 0.1% EDTA, and 1% β-mercaptoethanol. The proteolytic fragments were isolated by column chromatography on Sephadex G-100 in 4 M GdnHCl, 0.1 M Tris-HCl, pH 7.4, 0.01% EDTA, and 0.1% β-mercaptoethanol as described (Innerarity et al., 1983). The fractions corresponding to the 22-kDa (amino-terminal residues 1−191) and the 10-kDa (carboxyl-terminal residues 216−299) fragments were pooled, dialyzed against 5 mM NH_4HCO_3, and lyophilized. The fragments were solubilized in 0.1 M NH_4HCO_3 and stored at −20 °C.

Mutagenesis. The DNA for the production of the Thr57→Cys variant was prepared by PCR mutagenesis using mutagenic primers, as described (Dong et al., 1994). The variant protein was produced in *Escherichia coli* and isolated essentially as previously described (Lalazar et al., 1989). Following air oxidation, the nonreduced variant migrated at a slightly lower apparent molecular weight upon SDS−PAGE compared to a reduced sample of the apoE3 22-kDa fragment, demonstrating the formation of the expected disulfide bridge (data not shown).

Preparation of Phospholipid−Apolipoprotein Complexes. Complexes were prepared by incubation of the apolipoproteins with dimyristoylphosphatidylcholine (DMPC, Sigma) vesicles, at a DMPC/apolipoprotein ratio of 3:1 (w/w), at 25 °C for 16 h. The DMPC vesicles were obtained by sonicating the phospholipid under nitrogen for 3 × 7 min at 37 °C. Complexes with dipalmitoylphosphatidylcholine (DPPC, Sigma) and palmitoyllinoleoylphosphatidylcholine (PLPC, Sigma) at a phospholipid/apolipoprotein ratio of 3:1 (w/w) were prepared using the cholate dialysis procedure (Matz & Jonas, 1982). The mixture was incubated for 16 h at 43 °C for the complexes with DPPC and at 4 °C for those with PLPC. The cholate was removed by extensive dialysis.

The formation of the DMPC−apolipoprotein complexes was followed by monitoring the optical density decrease at 325 nm of multilamellar vesicles of DMPC with the apolipoproteins (phospholipid/apolipoprotein ratio of 2:1, w/w) as a function of temperature (Brasseur et al., 1990).

Complex Isolation and Characterization. Complexes were isolated by gel filtration on a Superose 6HR column in a 5 mM Tris-HCl buffer, pH 8.0, 0.15 M NaCl, and 0.2 g/L NaN_3, in an FPLC system (Waters). Complexes were detected by measuring the optical density at 280 nm and the Trp emission at 330 nm. The composition and size of the complexes were determined in the fraction with maximal ultraviolet absorption in the elution profile.

The chemical composition of the isolated complexes was assayed as follows: phospholipids were measured enzymatically using a commercially available kit (Biomérieux, Marcy-l'Etoile, France), and apolipoproteins were assayed by determination of the phenylalanine content by HPLC on a C18 reversed-phase column, after protein hydrolysis (Brasseur et al., 1990).

The sizes of the complexes were estimated by nondenaturing gel electrophoresis in an 8−25% polyacrylamide gradient (Pharmacia LKB PhastSystem). The gels were scanned using a laser densitometer (Pharmacia, Uppsala, Sweden), and the Stokes radii were estimated in comparison with protein standards (Pharmacia).

For electron microscopy examination, the complexes at an apolipoprotein concentration of 150 μg/mL were negatively stained with a 20 g/L solution of potassium phosphotungstate (pH 7.4). Sample aliquots of 7 μL were applied to Formvar carbon-coated grids and examined in a Zeiss EM 10C transmission electron microscope operating at 60 kV (Vanloo et al., 1992). Approximately 175 particles from each sample were measured, and the mean diameter and size distribution of the complexes were calculated. The number of apoE or apoE fragments per complex was calculated after cross-linking with bissulfosuccinimidylsuberate followed by electrophoresis on SDS gradient gels, according to the procedure of Swaney (1986).

Fluorescence Measurements. Fluorescence measurements were performed on an Aminco SPF-500 spectrofluorimeter

equipped with a special adapter (Aminco-J4-9501) for fluorescence polarization measurements (Vanloo et al., 1992). Complexes were labeled with diphenylhexatriene (DPH), and fluorescence polarization was measured as a function of temperature between 10 and 35 °C for the DMPC complexes and between 30 and 60 °C for the DPPC complexes.

Denaturation experiments were carried out by following the maximal emission wavelength of the Trp residues after exposure to increasing quantities of GdnHCl concentrations between 0 and 7 M.

Infrared Spectroscopy Measurements. Attenuated total reflection infrared spectroscopy (ATR-IR) was applied, as previously described, to determine the secondary structure of native and lipid-bound apolipoproteins as well as the relative orientation of the apolipoprotein helical segments and the phospholipid acyl chains (Goormaghtigh et al., 1987; Cabiaux et al., 1989). An aliquot of 70 μL of a solution with native apolipoprotein or with the complexes, containing 20 μg apolipoprotein in a 1 mM Tris-HCl buffer (pH 7.6), was spread on a germanium crystal plate. Deuteration of the sample was performed by flushing N_2, saturated with D_2O, into a sealed universal Perkin-Elmer sample holder at room temperature for 3 h, in order to avoid overlapping of the absorption bands for random and α-helical structures (Goormaghtigh et al., 1987).

Spectra were recorded on a Perkin-Elmer 1720X infrared spectrophotometer, using polarized incident light with a perpendicular (90°) and parallel (0°) orientation. A dichroic spectrum was obtained by subtracting the spectrum recorded with polarized light at 0° from that at 90°. The angle between a normal to the germanium crystal and the dipole is obtained from the calculation of the dichroic ratio $R^{ATR} = A_{90°}/A_{0°}$ (the ratio of the absorbances of the spectra recorded with polarized light at 90° and 0°). For each experiment up to 15 scans were stored and averaged.

Circular Dichroism Measurements. Circular dichroism (CD) spectra of the native apolipoproteins and of the complexes with phospholipids were measured at 23 °C in a Jasco 600 spectropolarimeter calibrated with a 0.1% (w/v) d_{10}-camphorsulfonic acid solution (Brasseur et al., 1990). Measurements were carried out at a protein concentration of 0.1 mg/mL in a 10 mM sodium phosphate buffer, pH 7.4. Nine spectra were collected and averaged for each sample. The percentage of α-helix was estimated from the ellipticity measurement at 222 nm by the following equation: % α-helix = $[([\theta]_{222} + 3000)/39\,000] \times 100\%$ (Morrisett et al., 1973), and also by curve-fitting on the entire ellipticity curve between 184 and 260 nm, according to the previously developed variable selection procedure (Johnson, 1990).

Purification of Lecithin:Cholesterol Acyltransferase. The LCAT was partially purified from the $d = 1.21-1.25$ g/mL fraction of normal human plasma by chromatography on Affi-Gel Blue and DEAE-Sephadex (Jonas, 1986). A final purification factor of 5100 was obtained for the enzyme. The remaining impurities, detected by SDS−PAGE in a 10−25% gradient gel (Laemmli, 1970) and by immunoblotting, consisted mainly of albumin. The enzyme was dialyzed against a 10 mM Tris-HCl buffer, pH 7.6, containing 5 mM EDTA and stored at −70 °C. Total protein levels were determined with the Bradford protein assay (Bradford, 1976), calibrated against an albumin standard. Scanning of the gels, after Coomassie Brilliant Blue staining, yielded an estimated LCAT concentration of 52 μg of enzyme/mL.

LCAT-Activation Properties of the Complexes. The LCAT activity in presence of the PLPC−cholesterol−apolipoprotein complexes was determined by HPLC measurement of the amount of cholesteryl esters (Vercaemst et al., 1989). We used PLPC complexes because their detection limit is lower than that of the DPPC complexes. The assay mixture consisted of variable amounts of complexes at cholesterol concentrations between 2 and 20 μM, 6 mM β-mercaptoethanol, and 90 μM defatted bovine serum albumin (BSA, Sigma). After 20-min preincubation at 37 °C, the enzymatic reaction was initiated by adding 5 μL of the semipurified LCAT enzyme (52 μg LCAT/mL) to 0.2 mL of the reaction mixture. The reaction was carried out at 37 °C and was stopped by extraction of the incubation mixture with hexane/isopropanol (3:2, v/v), containing cholesteryl heptadecanoate (Sigma) as an internal standard.

The HPLC separation was performed on a Hitachi 655A-11 liquid chromatograph equipped with a 655A-52 column oven and a Schoeffel SF-770 variable-wavelength detector. Samples were injected using the Bio-Rad (Model AS-100 HRLC) automatic sampling system. The separation was performed at 50 °C on a 5 μm Zorbax ODS reverse-phase column (250 × 4.6 mm inner diameter; Chrompack, Middelburg, the Netherlands). Cholesteryl esters were eluted isocratically at a flow rate of 1.2 mL/min with acetonitrile/isopropanol (1:1, v/v).

The course of the LCAT reaction was followed for 24 h, and the initial velocities were determined in the linear portion of the curves, i.e., between 0 and 15% cholesteryl ester formation for the PLPC−cholesterol−apoE3 complexes, between 0 and 3% for the PLPC/cholesterol complexes with the 22-kDa fragment and the 22-kDa Thr57→Cys variant, and between 0 and 30% for the PLPC−cholesterol−10-kDa fragment complexes. The initial reaction rates (V_o) were analyzed using a Lineweaver−Burke plot of $1/V_o$ versus $1/C$ according to Michaelis−Menten kinetics. A linear regression analysis yielded the apparent kinetic parameters: V_{max}, K_m, and V_{max}/K_m.

RESULTS

The formation of small discoidal complexes between the apolipoproteins and DMPC vesicles was monitored by measuring the decrease in turbidity at 325 nm as a function of temperature. A scan through the transition temperature of DMPC (Figure 1) showed a turbidity decrease due to a decrease in vesicular size and the formation of discoidal complexes. Intact apoE3 and the 10-kDa fragment have higher affinities for phospholipid than do the 22-kDa fragment and the 22-kDa Thr57→Cys variant. The lower amplitude of transition measured for the 22-kDa Thr57→Cys variant compared to the 22-kDa fragment suggests that the variant associates less tightly to phospholipids.

The complexes were fractionated on a Superose 6HR column for the DMPC−apolipoprotein complexes (Figure 2). Monitoring protein concentration by measuring Trp emission at 330 nm (Figure 2A) revealed the presence of unbound apolipoprotein in the DMPC−22-kDa fragment and DMPC−22-kDa Thr57→Cys variant mixtures. The 22-kDa wild-type fragment formed an heterogeneous complex with DMPC with a shoulder peak eluting at a smaller volume (Figure 2). The complex composition could be determined only on the major peak. Although the complex formed with

Table 1: Composition and Size of the DMPC−Apolipoprotein and DPPC−Apolipoprotein Complexes

complex	incubation mixture phospholipid/protein (weight ratio)	isolated complex phospholipid/protein (weight ratio)	isolated complex phospholipid/protein (molar ratio)	mol of protein per particle[a]	GGE[b] Stokes diameter (Å)	EM[c] diameter (Å)
DMPC−apoE3	3:1	3.1:1	156:1	2	115 ± 2	140 ± 22
DPPC−apoE3	3:1	3.3:1	152:1	2	116 ± 2	138 ± 19
DMPC−22-kDa	3:1	2.5:1	82:1	4	126 ± 2	160 ± 19
DPPC−22-kDa	3:1	2.0:1	61:1	4	119 ± 2	143 ± 16
DMPC−22-kDa Thr57→Cys	3:1	3.8:1	126:1			170 ± 19
DPPC−22-kDa Thr57→Cys	3:1	3.5:1	105:1			184 ± 22
DMPC−10-kDa	3:1	3.2:1	46:1	6	115−127 ± 2	154 ± 16
DPPC−10-kDa	3:1	2.7:1	36:1	6	110−116 ± 2	167 ± 19

[a] Obtained from cross-linking experiments. [b] Obtained from gradient gel electrophoresis (GGE) on nondenaturating gels by reference to standard proteins. The reproducibility of the diameter measurements is within ±2 Å. [c] Measured from electron micrographs obtained upon electron microscopy (EM) of negatively stained samples. Mean diameter ± SD is given for each complex (n = 175 for each group).

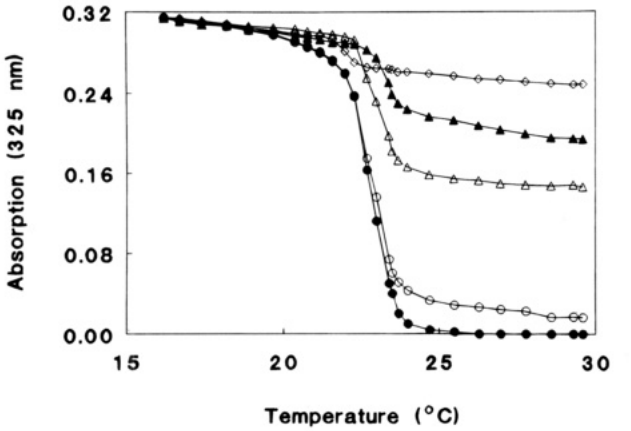

FIGURE 1: Interaction of various forms of apoE with DMPC. The ability of apoE3 or its thrombolytic fragments to complex with DMPC was monitored by absorption measurement at 325 nm as a function of temperature. (○) DMPC−apoE3; (△) DMPC−22-kDa fragment; (▲) DMPC−22-kDa Thr57→Cys variant; (●) DMPC−10-kDa fragment; (◇) DMPC.

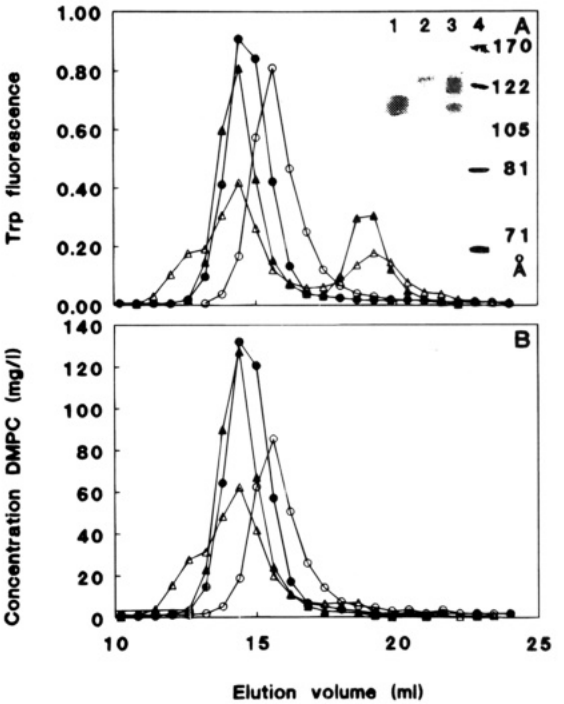

FIGURE 2: Superose 6 chromatography of apoE−DMPC complexes. Trp fluorescence intensity at 330 nm (A) and concentration of DMPC (mg/L) (B) were determined as a function of the elution volume for the DMPC−apolipoprotein mixtures. (○) DMPC−apoE3; (△) DMPC−22-kDa fragment; (▲) DMPC−22-kDa Thr57→Cys variant; (●) DMPC−10-kDa fragment. (Inset, A) Gradient gel electrophoresis of the complexes generated at an initial phospholipid/protein ratio of 3:1 (w/w). The complexes were isolated by gel chromatography on a Superose 6HR column. The electrophoretic separation was carried out in an 8−25% acrylamide gradient, and diameters were determined by comparison with known standards after scanning of the gels. Lane 1, DMPC−apoE3; lane 2, DMPC−22-kDa fragment; lane 3, DMPC−10-kDa fragment; lane 4, standards, in order of decreasing diameter, are thyroglobulin, ferritin, catalase, lactate dehydrogenase, and bovine serum albumin.

the 10-kDa fragment eluted as one peak, when the size of the complexes were determined by gradient gel electrophoresis on the top fraction of the elution peak, two fractions were resolved with respective diameters of 115 and 127 Å (Table 1). The complete composition listed in Table 1 corresponds to an average composition of these fractions as it was determined on the top fraction of the elution peak. Cross-linking experiments showed that the complexes generated with apoE3 and the 22- and 10-kDa fragments contain respectively 2, 4, and 6 molecules of protein per particle. On the basis of the helical content measured in the complexes, we estimated the number of helices for apoE3, the 22-, and 10-kDa fragments as 9, 5, and 3 per molecule. This corresponds to, respectively, 18, 20, and 18 helices surrounding the discoidal complex. Assuming a diameter of 15−17 Å per helix, these numbers correspond to the number of helical segments oriented parallel to the phospholipid acyl chains necessary to cover the edge of the discs (Jonas et al., 1993). Little if any free phospholipid appeared, since no peak was present in the void volume (Figure 2B).

The complex composition was determined by phospholipid and apolipoprotein quantitation in the fractions corresponding to the maximum peak of the elution pattern of the complex (Table 1). When expressed on a molar basis, the phospholipid/protein ratio in the phospholipid−apoE3 complexes was about 4 times higher than in complexes generated with the 10-kDa fragment. This phenomenon is probably due to the difference in molecular weight, since the weight ratio is about the same for both complexes. The composition of the complexes generated with the 22-kDa fragment and the corresponding variant were significantly different. The Thr57→Cys mutation results in the formation of a phospholipid-rich complex with a phospholipid/apolipoprotein ratio 1.5 times higher than that of complexes with the wild-type fragment (Table 1).

The size of the complexes was determined after gel filtration by gradient gel electrophoresis (GGE) (Figure 2A, inset, and Table 1), with the exception of the 22-kDa Thr57→Cys variant complexes, which dissociated during electrophoresis. The DMPC and DPPC complexes generated with the 10-kDa fragment were resolved into two bands,

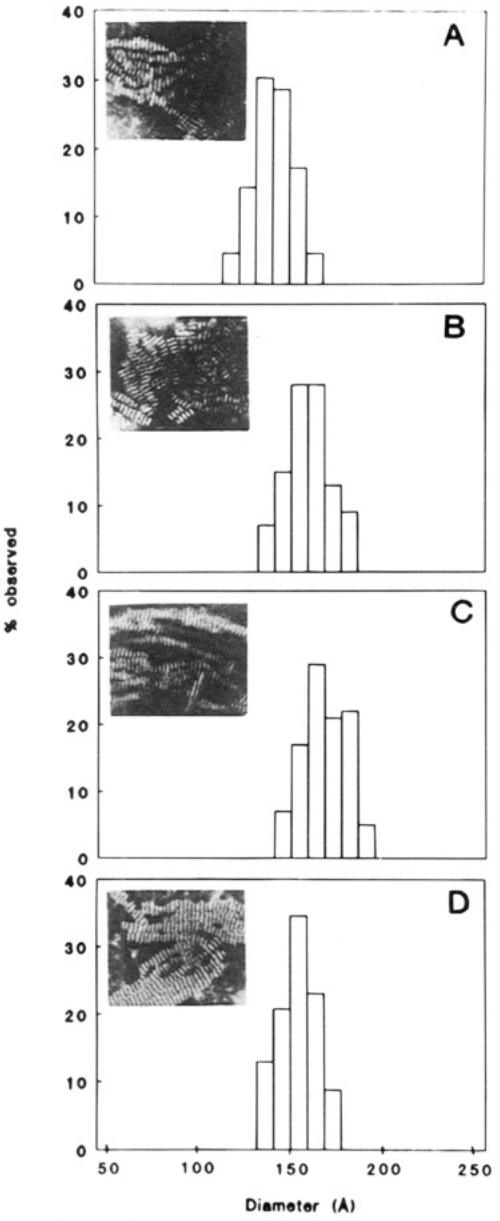

FIGURE 3: Size of the DMPC−apolipoprotein complexes determined by measuring the discs from the electron micrographs of the negatively stained complexes. (A) DMPC−apoE3; (B) DMPC−22-kDa fragment; (C) DMPC−22-kDa Thr57→Cys variant; (D) DMPC−10-kDa fragment.

corresponding to two complexes with diameters of 115−127 Å and 110−116 Å, respectively (Table 1).

The electron micrographs of the DMPC (Figure 3) and DPPC complexes (data not shown) revealed the typical pattern of rouleaux, characteristic of stacked discs. The diameters of the particles determined by both electron microscopy (EM) and GGE (Table 1) indicate that the intact apoE3 complexes are smaller than those of the thrombolytic fragments. When assessed by EM, the complexes appeared larger than they did by GGE, a phenomenon that has been previously observed with other apolipoproteins (Vanloo et al., 1991) (Table 1, Figure 2A, inset).

The degree of fluorescence polarization was measured after labeling of the isolated DMPC and DPPC complexes with DPH (Figure 4A,B). A decrease of the fluorescence polarization was observed between 10 and 35 °C for the DMPC complexes (Figure 4A), with transition temperatures at 25.5 °C for the apoE3, the 22-kDa fragment, and the 10-kDa fragment DMPC complexes and at 23.5 °C for the

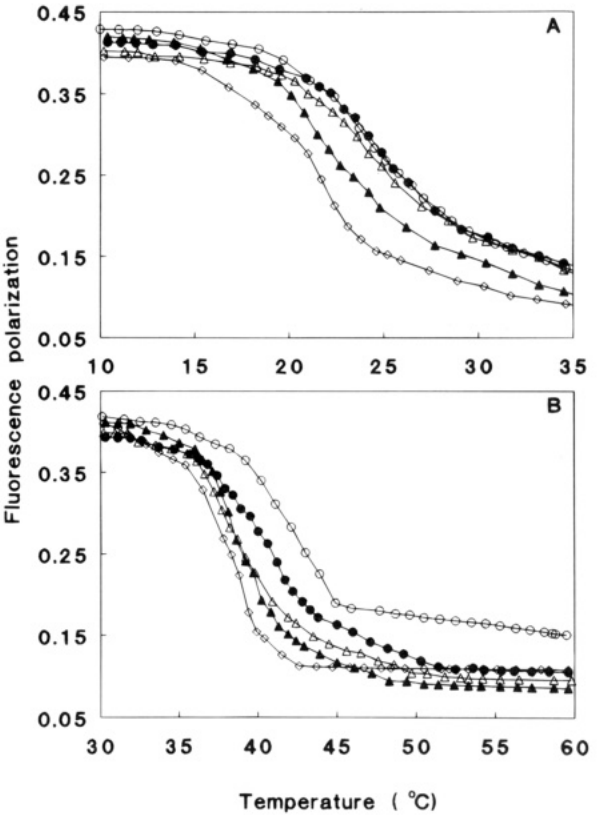

FIGURE 4: Fluorescence polarization decrease of phospholipid−apolipoprotein complexes as a function of temperature, after labeling with diphenylhexatriene. (A) (○) DMPC−apoE3; (△) DMPC−22-kDa fragment; (▲) DMPC−22-kDa Thr57→Cys variant; (●) DMPC−10-kDa fragment; (◇) DMPC. (B) (○) DPPC−apoE3; (△) DPPC−22-kDa fragment; (▲) DPPC−22-kDa Thr57→Cys variant; (●) DPPC−10-kDa fragment; (◇) DPPC.

Table 2: Maximum Trp Emission Wavelength and Denaturation by GdnHCl Followed by Measuring the Maximum Trp Emission Wavelength of the Native Apolipoproteins and the DMPC−Apolipoprotein and DPPC−Apolipoprotein Complexes

protein	maximum Trp emission wavelength (nm)	midpoint of denaturation curve (M GdnHCl)
ApoE3	343	1.2
DMPC−apoE3	337	2.4
DPPC−apoE3	337	2.6
22-kDa	342	1.9
DMPC−22-kDa	341	5.0
DPPC−22-kDa	341	5.0
22-kDa Thr57→Cys	343	2.0
DMPC−22-kDa Thr57→Cys	342	5.3
DPPC−22-kDa Thr57→Cys	341	5.8
10-kDa	341	1.0
DMPC−10-kDa	332	3.2
DPPC−10-kDa	333	3.9

DMPC−22-kDa Thr57→Cys variant complexes. The binding of the 22-kDa Thr57→Cys variant to DMPC had no effect on the DMPC transition temperature, which remained unchanged. The transition temperatures for the apoE3, 22-kDa fragment, the 22-kDa Thr57→Cys variant, and the 10-kDa fragment DPPC complexes (Figure 4B) were 41.5, 39.3, 39.3, and 41.0 °C, respectively.

The maximum Trp emission wavelengths of the native apolipoproteins and of the phospholipid−apolipoprotein complexes are summarized in Table 2. The blue-shift of the maximum Trp emission wavelength was most pronounced in the 10-kDa fragment (8 nm) and intact apoE3

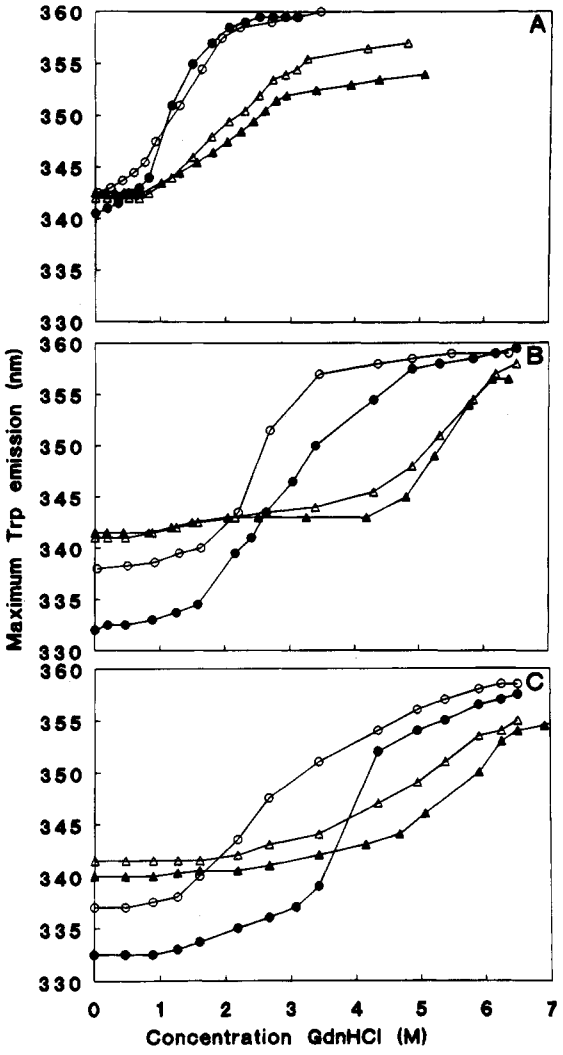

FIGURE 5: Denaturation of the native proteins, DMPC−apolipoprotein, and DPPC−apolipoprotein complexes monitored by measuring the maximum Trp emission wavelength at increasing GdnHCl concentrations. (A) (○) apoE3; (△) 22-kDa fragment; (▲), 22-kDa Thr57→Cys variant; (●) 10-kDa fragment. (B) (○) DMPC−apoE3; (△) DMPC−22-kDa fragment; (▲) DMPC−22-kDa Thr57→Cys variant; (●) DMPC−10-kDa fragment. (C) (○) DPPC−apoE3; (△) DPPC−22-kDa fragment; (▲) DPPC−22-kDa Thr57→Cys variant; (●) DPPC−10-kDa fragment.

complexes (6 nm). The wavelength was unchanged with the 22-kDa fragment and 22-kDa Thr57→Cys variant complexes (Table 2). Four of the seven Trp residues of intact apoE3, at positions 20, 26, 34, and 39 are in the 22-kDa fragment, and two, at positions 264 and 276, are in the 10-kDa fragment. Only these latter two Trp residues are sensitive to phospholipid binding, evidenced by the blue-shift in the phospholipid−10-kDa fragment complexes, as previously described (Aggerbeck et al., 1988).

The denaturation of the native and lipid-associated peptides was followed by monitoring the maximum Trp emission wavelength at increasing GdnHCl concentrations: as GdnHCl concentrations rose, the exposure of the Trp residues to the solvent increased, reflecting denaturation (Figure 5A−C). Association with lipids stabilizes and protects the protein structure against denaturation, as shown by the shift in the midpoint of denaturation toward higher GdnHCl concentrations in the complexes (Table 2). Intact apoE3 and the 10-kDa fragment denatured at lower GdnHCl concentrations than did the 22-kDa fragments; the denaturation midpoints

Table 3: Percentages of α-Helix Determined by Circular Dichroism and Infrared Measurements in the Native Apolipoproteins and DMPC−Apolipoprotein and DPPC−Apolipoprotein Complexes

	percentage α-helix		
protein	calculated from the molar ellipticity at 222 nm[a]	calculated from the CD spectra[b]	determined by IR
ApoE3	47	46	38
DMPC−apoE3	60	58	46
DPPC−apoE3	59	59	44
22-kDa	55	56	56
DMPC−22-kDa	49	50	47
DPPC−22-kDa	48	48	48
22-kDa Thr57→Cys	51	50	42
DMPC−22-kDa Thr57→Cys	63	60	47
DPPC−22-kDa Thr57→Cys	60	60	44
10-kDa	52	51	42
DMPC−10-kDa	57	54	42
DPPC−10-kDa	58	54	45

[a] Calculated according to Morrisett et al. (1973). [b] Calculated according to Johnson (1990).

were 1.2 and 1.0 M, respectively, compared to 1.9 and 2.0 M, suggesting that the conformation of the carboxyl-terminal domain was less structured than that of the amino-terminal domain, a finding consistent with previous observations (Aggerbeck et al., 1988; Wetterau et al., 1988). The conformation of the 22-kDa Thr57→Cys variant was further stabilized by the Cys57−Cys112 disulfide bond, so that an even higher GdnHCl concentration was required for denaturation.

The percentage of α-helical structure in the native apolipoproteins and in the complexes, as obtained by infrared spectroscopy and circular dichroism, is summarized in Table 3. Phospholipid binding increased the α-helical content, especially in intact apoE3, whereas there was a slight decrease in the α-helical content of the 22-kDa fragment.

The dichroic ratio R^{ATR}, calculated from the ATR-IR measurements with polarized light, indicated that the phospholipid hydrocarbon chains of the complexes were tilted at an angle of about 20° from the normal to the germanium surface, compared with an average angle of about 27° for the long axis of the α-helices of the peptides. From these data, we could therefore assume that the helices of the apolipoproteins and the phospholipid acyl chains were oriented parallel to each other.

The kinetics of the LCAT reaction using the discoidal PLPC−cholesterol−apolipoprotein complexes as substrates were followed for 24 h (Figure 6, inset: between 0 and 0.5 h). The percentage of esterified cholesterol was highest for the substrate consisting of discoidal PLPC−cholesterol−10-kDa fragment complexes. Saturable kinetics were observed at 3 h with the phospholipid−cholesterol−10-kDa fragment complexes, compared with 16 h for apoE3. In both cases, cholesterol esterification exceeded 90% after 24 h. For the PLPC−cholesterol−22-kDa fragment and PLPC−cholesterol−22-kDa Thr57→Cys variant complexes, cholesterol esterification reached 36% and 22%, respectively, after 24 h.

A reciprocal plot of the initial maximal velocity, for up to 15% and 30% esterification of the complexes with apoE3 and the 10-kDa fragment, respectively, as a function of the inverse of the cholesterol concentration, is shown in Figure 7. As expected from the comparison of the initial linear

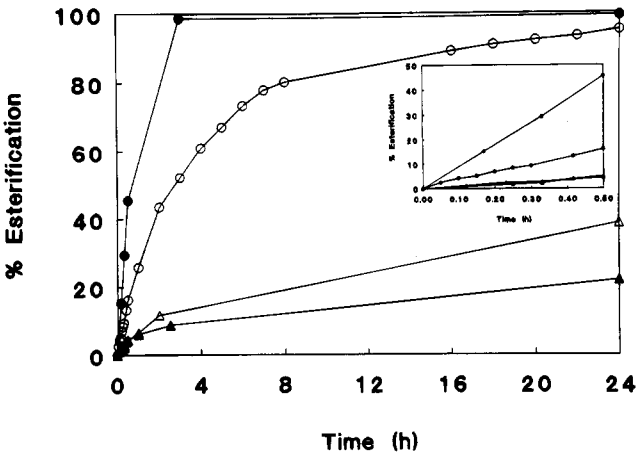

FIGURE 6: Activation of the LCAT reaction with discoidal PLPC–cholesterol–apolipoprotein complexes between 0 and 24 h (inset between 0 and 0.5 h). (○) PLPC–cholesterol–apoE3; (△) PLPC–cholesterol–22-kDa fragment; (▲) PLPC–cholesterol–22-kDa Thr57→Cys variant; (●) PLPC–cholesterol–10-kDa fragment.

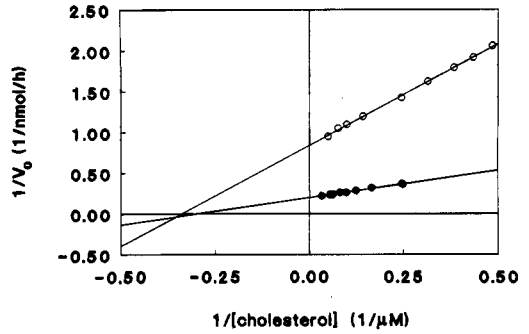

FIGURE 7: Lineweaver–Burke plots giving the inverse of the initial velocity ($1/V_o$) as a function of the inverse of the substrate concentration (1/concentration of cholesterol) for the reaction of LCAT with the PLPC–cholesterol–apolipoprotein complexes. (○) PLPC–cholesterol–apoE3; (●) PLPC–cholesterol–10-kDa fragment.

Table 4: Apparent Kinetic Constants of the LCAT Reaction with Discoidal Complexes Generated between PLPC–Cholesterol and apoE3, the 22-kDa Fragment, the 22-kDa Thr57→Cys Variant, and the 10-kDa Fragment

complex	V_o (nmol/h)	V_{max} (nmol/h)	K_m (μM)	V_{max}/K_m (nmol h^{-1} μM^{-1})
PLPC–cholesterol–apoE3	0.9	1.2	2.6	0.5
PLPC–cholesterol–22-kDa	0.2	–[a]	–[a]	–
PLPC–cholesterol–22-kDa Thr57→Cys	0.3	–[a]	–[a]	–
PLPC–cholesterol–10-kDa	2.7	4.9	3.3	1.5

[a] For the 22-kDa fragment and the 22-kDa Thr57→Cys variant, the reaction rate was too low for an accurate determination of the reaction parameters.

portions of the curves shown in Figure 6, V_{max} was higher for the PLPC–cholesterol–10-kDa fragment complexes (4.9 nmol of cholesteryl ester/h) than for the PLPC–cholesterol–apoE3 complexes (1.2 nmol/h) (Table 4). The K_m value, expressed as cholesterol concentration, was about the same for the PLPC–cholesterol–10-kDa fragment complexes and the complexes with apoE3 (3.3 and 2.6 μM, respectively). Consequently, a higher substrate efficiency, expressed as V_{max}/K_m, was observed for the PLPC–cholesterol complexes with the 10-kDa fragment than with apoE3: 1.5 and 0.5 nmol of cholesteryl esters h^{-1} (μM cholesterol)$^{-1}$, respectively. For the 22-kDa fragment and the 22-kDa Thr57→Cys variant, the reaction rate was too low for an accurate determination of the kinetic parameters.

DISCUSSION

The interaction of apoE3 with the LDL receptor of fibroblasts requires it to be lipid-associated (Innerarity et al., 1979). In an attempt to characterize the lipid-binding and LCAT-activating domains of apoE3, we compared the properties of its two major thrombolytic fragments—residues 1–191 (22-kDa fragment) and residues 216–299 (10-kDa fragment)—as well as a 22-kDa Thr57→Cys variant, in which a disulfide cross link between helices 2 and 3 of the four-helix bundle of this domain had been introduced.

Turbidity measurements showed that apoE3 and the 10-kDa fragment bind phospholipids with higher affinity than does either 22-kDa fragment. The lower affinity of the 22-kDa Thr57→Cys variant for phospholipids was further demonstrated by the lower transition temperature determined by fluorescence polarization.

The diameter of the DMPC–apoE complexes (2.5:1, w/w) measured in this study is in agreement with the value of 150 ± 15 Å reported by Lund-Katz et al. (1993) from electron microscopy measurements.

Our results for the Trp fluorescence emission compare well with those reported by Aggerbeck et al. (1988), who found a pronounced blue-shift of the fluorescence emission for apoE3 and the 10-kDa fragment upon lipid binding and a smaller shift for the 22-kDa fragment. The shift for apoE3 is intermediate between those of the 22-kDa fragment and the 10-kDa fragment, reflecting the change of Trp to a more apolar environment. The blue-shift of the 10-kDa fragment suggests that the Trp-containing region of the carboxyl-terminal domain becomes further shielded by the lipid environment (Aggerbeck et al., 1988), although Trp residues 264 and 276 might have already been partially shielded by self-association of the lipid-free apolipoprotein. The blue-shift of apoE3 probably reflects that of the carboxyl-terminal domain and is consistent with a major role for the 10-kDa fragment in the interaction of apoE3 with phospholipids.

Wetterau et al. (1988) monitored the denaturation by GdnHCl of apoE3 and its thrombolytic fragments by circular dichroism and observed a biphasic curve indicating that the unfolding of apoE3 occurs through stable intermediates. When following the GdnHCl denaturation of apoE3 by Trp emission wavelength measurement, we did not obtain a biphasic curve. Circular dichroism measurements, monitoring the change of secondary structure, might be more sensitive to intermediate states than fluorescence measurements, which monitor only the exposure of the Trp residues to the solvent. The transition midpoint of the denaturation of the 10- and 22-kDa fragments as assessed by CD measurement is 0.7 and 2.5 M, respectively (Wetterau et al., 1988); these values are comparable to those obtained by Trp fluorescence measurement. The 57–112 disulfide bridge further protects the amino-terminal domain against denaturation. The unusually high stability of the amino-terminal domain may be related to its receptor-binding function (Innerarity et al., 1983) and is probably due to its highly organized globular structure.

The percentages of α-helix measured for apoE3 and for the fragments are slightly lower than those reported by Aggerbeck et al. (1988). The α-helical content of apoE and of the 10-kDa fragment increased upon phospholipid binding,

in agreement with data from Jonas et al. (1993) and Lund-Katz et al. (1993) for apoE−DMPC complexes. This supports the hypothesis that the C-terminal domain of apoE contains the primary lipid-binding site.

The V_{max} value of 1.2 nmol of cholesteryl ester/h for the LCAT reaction with PLPC−cholesterol−apoE3 complexes is comparable to the value of 0.142 found by Jonas et al. (1993) for the corresponding complexes with palmitoyloleoylphosphatidylcholine, as we used a 10-fold higher concentration of the LCAT enzyme. According to the composition of the PLPC−cholesterol−apoE3 complexes (data not shown), the K_m value is 2.6 expressed as μM cholesterol. The corresponding value, expressed as apoE3 concentration, is 0.21 μM, which is in agreement with the 0.19 μM found by Jonas et al. (1993).

Westerlund and Weisgraber (1993) studied a series of carboxyl-terminally truncated variants of apoE to define more precisely the regions of this domain responsible for its lipid-binding properties. The results demonstrate that deletion of residues 267−299 impairs association of apoE with lipoprotein particles, suggesting that these residues are essential for lipid binding. Extended studies (Dong et al., 1994) subsequently demonstrated that only up to residue 272 is required for complete lipoprotein association.

Apolipoprotein E3 contains two structural domains that are modeled by the 22- and 10-kDa thrombolytic fragments. As shown by GdnHCl denaturation, the amino-terminal fragment is relatively stable, more closely resembling that of globular proteins than of other apolipoproteins. Although it associates poorly with native lipoproteins (Weisgraber, 1990), this fragment is capable of associating with phospholipid, forming discoidal complexes. The present studies suggest that this association with phospholipid likely results in the reorientation of the helical segments to form antiparallel 17-residue helices, as has been demonstrated for other apolipoproteins (Brasseur et al., 1992). When this reorientation is impaired by linkage of helices 2 and 3 through a disulfide bridge, lipid binding is hampered. In contrast to the amino-terminal domain, the carboxyl-terminal domain of apoE3 is structurally less stable, as it denatures at low GdnHCl concentration, typical for apolipoproteins (Tall et al., 1976). The carboxyl-terminal fragment binds avidly to lipids, and it is further responsible for the LCAT-activating properties of apoE. Although a reorientation of the long helices of the N-terminal fragment is required for optimal lipid binding, this does not substantially improve the LCAT activation properties of the complex generated with the 22-kDa fragment. This observation suggests that besides a particular structure of the discoidal apoprotein−lipid complex, specific residues or stretches of residues in the cofactor protein might be required for activation. This is supported by recent data on apoA-I (Jonas et al., 1993; Calabresi et al., 1993) and on apoA-IV (Emmanuel et al., 1994).

ACKNOWLEDGMENT

We are grateful to G. Michiels, C. Tilleman, J. Taveirne, H. Caster, T. Simmons, and Y. Newhouse for their excellent technical assistance, K. Humphrey for manuscript preparation, and L. DeSimone and D. Levy for editorial assistance.

REFERENCES

Aggerbeck, L. P., Wetterau, J. R., Weisgraber, K. H., Wu, C.-S. C., & Lindgren, F. T. (1988) *J. Biol. Chem. 263*, 6249−6258.

Bradford, M. M. (1976) *Anal. Biochem. 72*, 248−254.

Brasseur, R., De Meutter, J., Vanloo, B., Goormaghtigh, E., Ruysschaert, J. M., & Rosseneu, M. (1990) *Biochim. Biophys. Acta 1043*, 245−252.

Brasseur, R., Lins, L., Vanloo, B., Ruysschaert, J.-M., & Rosseneu, M. (1992) *Proteins 13*, 246−257.

Cabiaux, V., Brasseur, R., Wattiez, R., Falmagne, P., Ruysschaert, J.-M., & Goormaghtigh, E. (1989) *J. Biol. Chem. 264*, 4928−4938.

Calabresi, L., Meng, Q.-H., Castro, G. R., & Marcel, Y. L. (1993) *Biochemistry 32*, 6477−6484.

Chen, C. H., & Albers, J. J. (1985) *Biochim. Biophys. Acta 836*, 279−285.

Dong, L.-M., Wilson, C., Wardell, M. R., Simmons, T., Mahley, R. W., Weisgraber, K. H., & Agard, D. A. (1994) *J. Biol. Chem. 269*, 22358−22365.

Eisenberg, S. (1984) *J. Lipid Res. 25*, 1017−1058.

Emmanuel, F., Steinmetz, A., Rosseneu, M., Brasseur, R., Gosselet, N., Attenot, F., Cuiné, S., Séguret, S., Latta, M., Fruchart, J.-C., & Denèfle, P. (1994) *J. Biol. Chem. 269*, 29883−29890.

Goormaghtigh, E., Brasseur, R., Huart, P., & Ruysschaert, J. M. (1987) *Biochemistry 26*, 1789−1794.

Gordon, V., Innerarity, T. L., & Mahley, R. W. (1983) *J. Biol. Chem. 258*, 6202−6212.

Innerarity, T. L., Pitas, R. E., & Mahley, R. W. (1979) *J. Biol. Chem. 254*, 4186−4190.

Innerarity, T. L., Friedlander, E. J., Rall, S. C., Jr., Weisgraber, K. H., & Mahley, R. W. (1983) *J. Biol. Chem. 258*, 12341−12347.

Johnson, W. C., Jr. (1990) *Proteins 7*, 205−214.

Jonas, A. (1984) *Exp. Lung Res. 6*, 255−270.

Jonas, A. (1986) *J. Lipid Res. 27*, 689−698.

Jonas, A., Steinmetz, A., & Churgay, L. (1993) *J. Biol. Chem. 268*, 1596−1602.

Koo, C., Innerarity, T. L., & Mahley, R. W. (1985) *J. Biol. Chem. 260*, 11934−11943.

Laemmli, U. K. (1970) *Nature 227*, 680−685.

Lalazar, A., Ou, S.-H. I., & Mahley, R. W. (1989) *J. Biol. Chem. 264*, 8447−8450.

Lund-Katz, S., Weisgraber, K. H., Mahley, R. W., & Phillips, M. C. (1993) *J. Biol. Chem. 268*, 23008−23015.

Mahley, R. W., & Innerarity, T. L. (1983) *Biochim. Biophys. Acta 737*, 197−222.

Matz, C. E., & Jonas, A. (1982) *J. Biol. Chem. 257*, 4535−4540.

McLean, J. W., Elshourbagy, N. A., Chang, D. J., Mahley, R. W., & Taylor, J. M. (1984) *J. Biol. Chem. 259*, 6498−6504.

Morrisett, J. D., David, J. S. K., Pownall, H. J., & Gotto, A. M., Jr. (1973) *Biochemistry 12*, 1290−1299.

Rall, S. C., Jr., Weisgraber, K. H., & Mahley, R. W. (1982) *J. Biol. Chem. 257*, 4171−4178.

Swaney, J. B. (1986) *Methods Enzymol. 128*, 613−626.

Tall, A. R., Shipley, G. G., & Small, D. M. (1976) *J. Biol. Chem. 251*, 3749−3755.

Tall, A. R., Small, D. M., Deckelbaum, R. J., & Shipley, G. G. (1977) *J. Biol. Chem. 252*, 4701−4711.

Vanloo, B., Morrison, J., Fidge, N., Lorent, G., Lins, L., Brasseur, R., Ruysschaert, J.-M., Baert, J., & Rosseneu, M. (1991) *J. Lipid Res. 32*, 1253−1264.

Vanloo, B., Taveirne, J., Baert, J., Lorent, G., Lins, L., Ruyschaert, J.-M., & Rosseneu, M. (1992) *Biochim. Biophys. Acta 1128*, 258−266.

Vercaemst, R., Union, A., Rosseneu, M., De Craene, I., De Backer, G., & Kornitzer, M. (1989) *Atherosclerosis 78*, 245−250.

Weisgraber, K. H. (1990) *J. Lipid Res. 31*, 1503−1511.

Weisgraber, K. H. (1994) *Adv. Protein Chem. 45*, 249−302.

Weisgraber, K. H., Rall, S. C., Jr., & Mahley, R. W. (1981) *J. Biol. Chem. 256*, 9077−9083.

Westerlund, J. A., & Weisgraber, K. H. (1993) *J. Biol. Chem. 268*, 15745−15750.

Wetterau, J. R., Aggerbeck, L. P., Rall, S. C., Jr., & Weisgraber, K. H. (1988) *J. Biol. Chem. 263*, 6240−6248.

Wilson, C., Wardell, M. R., Weisgraber, K. H., Mahley, R. W., & Agard, D. A. (1991) *Science 252*, 1817−1822.

Zannis, V. I., McPherson, J., Goldberger, G., Karathanasis, S. K., & Breslow, J. L. (1984) *J. Biol. Chem. 259*, 5495−5499.

BI950183F